CHARACTERIZATION AND MECHANICAL PROPERTIES OF SINTERED CLAY MINERALS

SARA TOMINC,[1] VILMA DUCMAN,[1] JAKOB KÖNIG,[2] SREČO ŠKAPIN,[2] MATJAŽ SPREITZER[2]

[1] Slovenian National Building and Civil Engineering Institute, Ljubljana, Slovenia
sara.tominc@zag.si, vilma.ducman@zag.si
[2] Jožef Stefan Institute, Ljubljana, Slovenia
jakob.konig@ijs.si, sreco.skapin@ijs.si, matjaz.spreitzer@ijs.si

The need to reduce energy consumption and the carbon footprint generated by firing ceramics has stimulated research to develop sintering processes carried out at lower temperatures (ideally not above 300 °C) and high pressures (up to 600 MPa), the so-called cold sintering process (CSP) (Grasso et al., 2020, Maria et al., 2017). To evaluate the applicability of CSP to clays, we focused on two representative clay minerals, kaolinite and illite, and on the natural clay material obtained from a Slovenian brick manufacturer. The selected clay materials were characterized on the basis of mineralogical-chemical composition (XRD, XRF) and particle size distribution (SEM analysis, PSD, BET). The powders of clay minerals and natural clay material were first sintered in a heating microscope to determine the sintering conditions and then in a laboratory furnace at 1100 °C for 2 hours and additionally at 1300 °C for kaolinites. The effect of compression of the initial powders on their final properties was also investigated.

DOI
https://doi.org/10.18690/um.fkkt.1.2024.10

ISBN
978-961-286-829-1

Keywords:
conventional sintering,
cold sintering,
clay minerals,
characterization,
mechanical properties

University of Maribor Press

1 Introduction

The cold sintering process (CSP) is a process in which an inorganic powder is densified in the presence of a transient liquid phase as a phase fraction between 1-10% by volume (Maria et al., 2017). The main goal of this process is to reduce the energy consumption, processing time, cost and carbon footprint generated by conventional sintering processes (Galotta et al., 2021, Grasso et al., 2020). CSP was developed at Pennsylvania State University by Prof. Clive Randall and his research team (also known as the Randall`s method) and first applied for a patent in 2015 (Galotta et al., 2021, Grasso et al., 2020).

The low temperature (< 300 °) C and high pressure (up to 600 MPa) of CSP enable a considerable reduction in the energy and costs required for the consolidation of ceramic powder. The low temperature is not only advantageous from an energy point of view, but also because it drastically reduces the possibility of unwanted phase transformation during the sintering process (Galotta et al., 2021, Grasso et al., 2020, Guo et al., 2016). The synergy between the externally applied pressure, the limited temperature and the added liquid phase enables the successful production of dense materials in a short time with a large energy saving compared to other sintering techniques. Although cold sintering is already widely used, the densification mechanisms are not yet clearly understood (Galotta et al., 2021).

In order to compare the CSP approach with clays, a reference study was first carried out on the conventional sintering of kaolinite, illite and natural clay material so that the success of the samples produced with CSP could be evaluated later. Kaolinite and illite are common clay minerals found in nature and used for various applications (Gianni et al., 2020, Zhang et al., 2022). Kaolinite is of particular interest as it undergoes dehydroxylation to an amorphous state (forming metakaolin), which is stable over a wide temperature range (Michot et al., 2008). The natural clay material used for the production of clay bricks was taken from the production line just before the molding stage to ensure an industrially suitable clay sample.

2 Materials and methods

Representative clay mineral kaolinite-low defect (Kl) (Warren Country Georgia USA, KGa-1b, 125 grams/unit), kaolinite-high defect (Kh) (Warren Country Georgia USA, KGa-2, 125 grams/unit), illite (Il) (ilite-smectite mixed layer (70/30 ordered), Slovakia ISSCz-1, 50 grams/unit) and representative natural clay material (Cl) from the Slovenian brick manufacturer were selected.

For chemical analysis, samples were sieved below 125 μm and dried at 105 °C. The loss on ignition (LOI) was determined at 950 °C. A fused bead was then prepared with a mixture of sample and flux (50% lithium tetraborate/50% lithium metaborate) at a ratio of 1:10 (0.947 g: 9.47 g) and heated at 1100 °C. The chemical composition was determined using an ARL PERFORM'X wavelength dispersive X-ray fluorescence spectrometer (WDXRF; Thermo Fischer Scientific Inc., Ecublens, Switzerland) with a Rh-target X-ray tube and UniQuant 5 software (Thermo Fisher Scientific Inc., Waltham, MA, USA). Mineralogical analyses were performed using a Bruker AXS D4 Endeavor (Bruker, Bilelrica, MA) X-ray diffractometer equipped with Cu Kα radiation with a step size of 0.04° from angles 5-70°. The XRD patterns were solved using EVA software.

The specific surface area was determined by the Brunauer–Emmett–Teller (BET) method using a Micromeritics ASAP-2020 analyzer (Micromeritics, Norcross, GA, USA). The shape and size of the clay mineral particles were determined by field emission scanning electron microscopy (FE-SEM, Carl Zeiss ULTRA Plus, Oberkochen, Germany). The particle size distribution (PSD) of the samples was measured by laser diffraction granulometry using a Sync + FlowSync laser grain size analyzer (Microtrack MRB) in wet dispersion (dH_2O) measurement mode.

Prior to sintering, the densification characteristics of the samples were recorded using a heating microscope (Hesse Instruments, Osterode am Harz, Germany). The densification curves were recorded up to 1200 °C for Cl, 1280 °C for Il and 1400 °C for Kh and Kl with a heating rate of 10 °C/min. Kaolinite, illite and natural clay material were then ground to a grain size below 63 μm and pressed uniaxially at a pressure of 150 MPa to form 10 mm thick pellets with a diameter of 10 mm. The samples were sintered in a laboratory furnace PLF 160/9 (Protherm, Ankara, Turkey) at 1100 °C and 1300 °C for 2 hours with heating/cooling rates of 150 °C/h.

The open porosity of the sintered clay materials was determined by mercury intrusion porosimetry (MIP). Small representative pellets with a diameter and height of 10 mm were analysed immediately after sintering using the Micromeritics® Autopore IV 9500 instrument (Micromeritics, Norcross, GA, USA). The compressive strength was measured using a ToniTROL compressive strength testing machine (ToniTechnik, Berlin, Germany) at a force rate of 1.2 kN/s.

XRadia CT-400 tomography (XRadia, Concord, California, USA) was used to determine the pellets produced with CSP. The spatial resolution per pixel was 22.5 μm, equipped with a 0.39x optical objective. The voltage and current were set to 80kV and 87 μA respectively. 1600 projection images with an exposure time of 1 second per projection were captured through the charge-coupled device (CCD) camera. Avizo software (Thermo Fisher) was used for density-based segmentation and 3D reconstruction.

3 Results and Discussion

3.1 Characterization

XRF analysis of the clay minerals and natural clay material showed that they are mainly composed of Al_2O_3, SiO_2 and Fe_2O_3, with minor contents of CaO, MgO, K_2O and TiO_2. The average values of the primary oxides measured by XRF, LOI at 950 °C (Figure 1) and BET are given in Table 1.

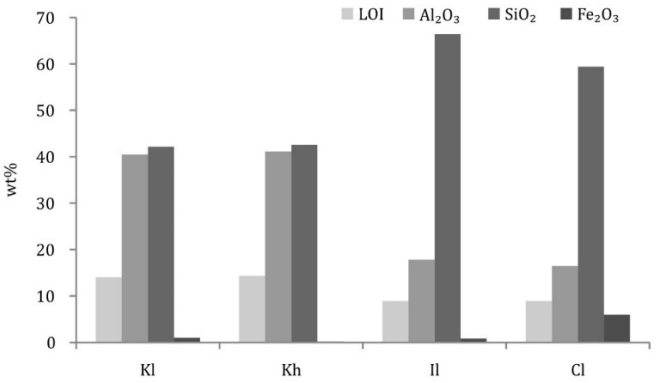

Figure 1: Comparison of LOI and primary oxides by XRF analysis
Source: own.

Table 1: BET, LOI at 950 °C and chemical composition of the clays in terms of primary oxides (wt%), measured using XRF.

Sample	BET (m^2/g)	LOI (950 °C)	Al_2O_3	SiO_2	Fe_2O_3	CaO	MgO	K_2O	TiO_2
Kl	19.85	14.05	40.48	42.15	0.98	0.02	0.06	0.04	1.92
Kh	11.15	14.31	41.13	42.58	0.19	0.03	/	0.01	1.44
Il	38.55	8.95	17.84	66.44	0.83	0.20	1.56	3.81	0.10
Cl	26.88	9.94	16.46	59.38	5.97	3.21	1.67	2.34	0.03

The phase composition of the samples was analyzed using powder XRD. Figure 2 shows that the kaolinites Kl and Kh have a XRD pattern typical of kaolinite. However, Kl has more pronounced reflections in the range 2 Θ =19-24° than Kh, indicating a higher degree of crystalline order. The Hinckley index for Kl is 0.98, while for Kl it is 0.41. XRD analysis of Il and Cl showed that the clay also contains quartz (Q), while Cl also contains zeolite (Z), illite (I), muscovite (M), kaolinite (K) and calcite (C).

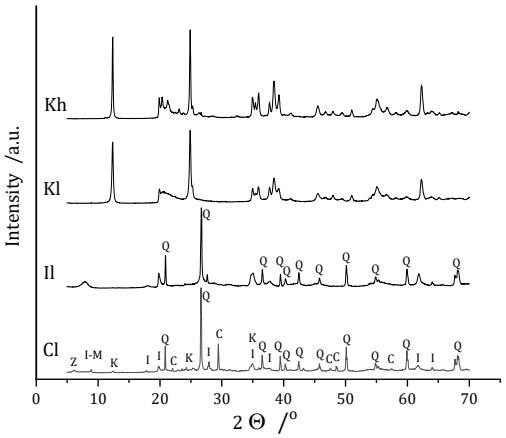

Figure 2: X-ray diffraction patterns of selected samples

Source: own.

In the next step, we examined the microstructural features of the samples using the SEM. We observed the presence of kaolinite "booklets", i.e. micron-sized morphological structures composed of numerous platelets typical of the mineral kaolinite (Balan et al., 2014), as well as fine kaolinite particles (Figure 3a, b), curled illite leaves (Figure 3c) and large particles of natural clay material (Figure 3d).

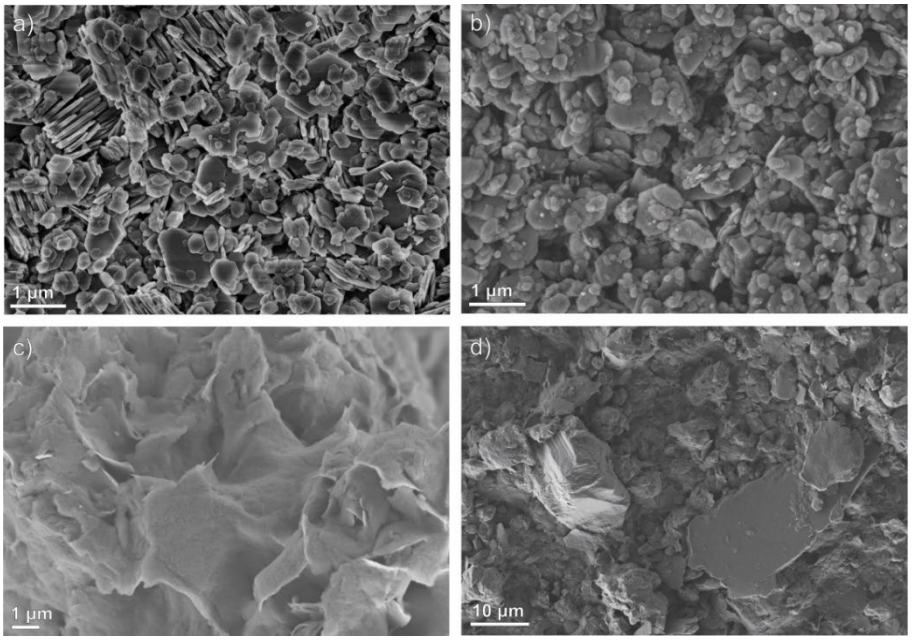

Figure 3: SEM images of a) Kl, b) Kh, c) Il and d) Cl
Source: own.

In addition, the measurement of PSD showed that the fineness of the clay minerals was greater in Kl and Kh than in Il and Cl (Figure 4).

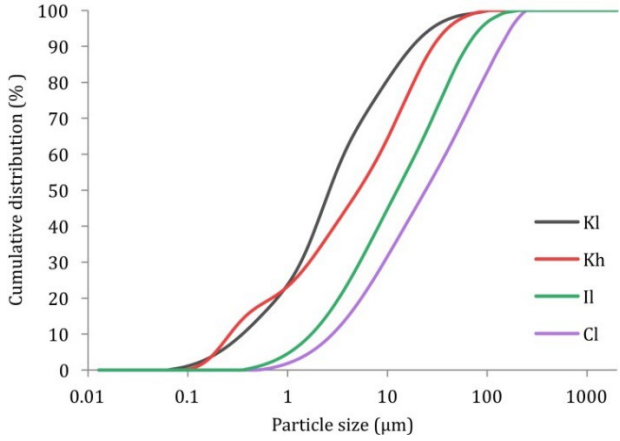

Figure 4: Cumulative distribution (% passing, based on volume) of selected samples
Source: own.

In order to determine the optimum sintering temperature, the densification behavior of our samples was measured using a heating- stage microscope. The relative shrinkage (%) of the samples as a function of temperature is shown in Figure 5. Cl reaches the peak of the densification rate at 1160 °C, Il at 1250 °C, while the onset of densification of Kl and Kh occurs at higher temperatures and the maximum rate is reached at 1320 °C for Kh and 1400 °C for Kl. In accordance with the densification behavior, the sintering temperature was set at 1100 °C for all samples and at 1300 °C for Kl and Kh.

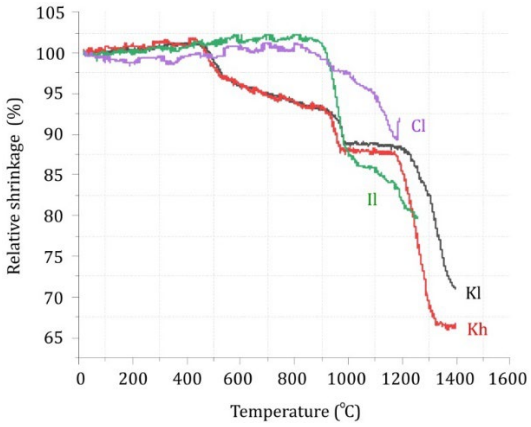

Figure 5: Relative shrinkage of the Kl, Kh, Il and Cl as a function of temperature
Source: own.

3.2 Mechanical properties

In the last step, we addressed the mechanical properties of the sintered clay minerals. At a sintering temperature of 1100 °C, the densification of Cl and Il is intensive, while a higher temperature was required for Kh and Kl. The compressive strength was measured on five pellets of each sample after sintering at 1100 °C and at 1300 °C for Kl and Kh. The results are shown in Table 2 and Figure 6.

The total porosity of the samples sintered at 1100 °C was between 11 and 40%. The porosity of the kaolinites was significantly lower with increasing sintering temperature up to 1300 °C. At 1300 °C, Kh and Kl showed significantly lower porosity (~4-5%), which is consistent with the higher mechanical strength and density of these samples.

Table 2: Geometric density, bulk density and porosity, measured with MIP, and compressive strength of selected samples, sintered at 1100 and 1300 °C.

Sample	Temp. (°C)	Bulk density (g/cm³)	Geom. density (g/cm³)	Porosity (%)	Compressive strength (MPa)
Kl	1100	1.66	1.45	39.5	5.6 ± 2.0
	1300	2.58	2.57	4.6	340.9 ± 36.8
Kh	1100	1.81	1.75	31.1	35.5 ± 8.0
	1300	2.68	2.68	4.3	74.0 ± 36.8
Il	1100	2.21	2.19	13.9	160.5 ± 6.2
Cl	1100	2.26	2.27	11.0	303.3 ± 31.9

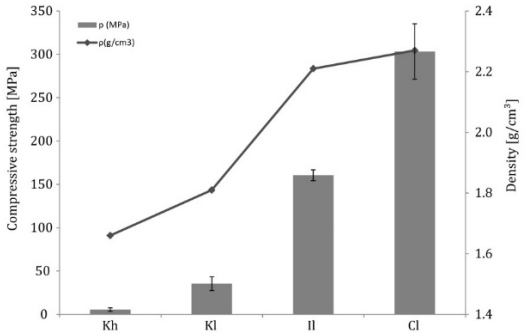

Figure 6: Compressive strengths and bulk densities of clay materials after conventional sintering at 1100 °C for 2 hours

Source: own.

The porosity values and the bulk density of the samples, measured with the MIP, are listed in Table 2. The pore size distribution ranged from 0.01 to 100 µm, as shown in Figure 7.

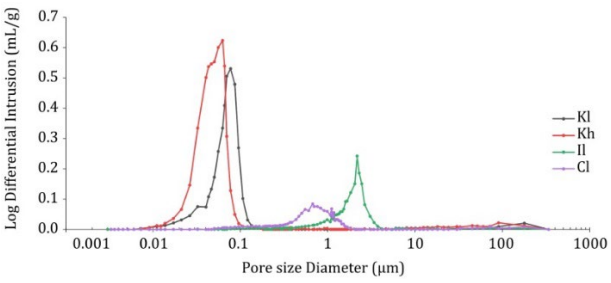

Figure 7: Differential mercury intrusion porosimetry of sintered clay minerals

Source: own.

In addition, a series of samples will be prepared using CSP under different conditions in the typical range of CSP. Preliminary results show that the Cl pellet was successfully prepared using CSP at a temperature of 240 C, a pressure of 500 MPa and a processing time of 3 minutes (Figure 8).

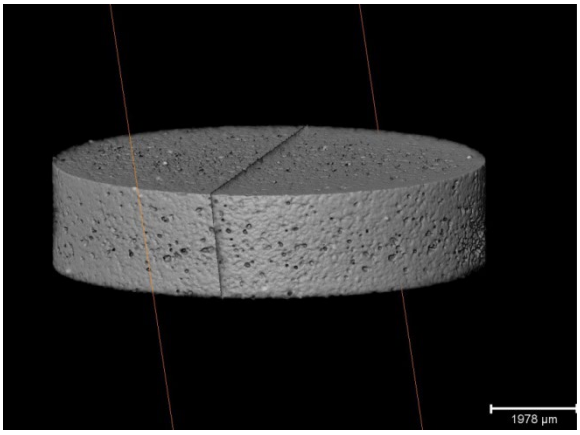

Figure 8: 3D view with cross-section of the Cl pellet prepared using CSP at a temperature of 240°C, a pressure of 500 MPa and a processing time of 3 minutes

Source: own.

4 Conclusions

In this study, selected clay minerals and the natural clay material were characterized and then conventionally sintered at 1100 and 1300 °C for 2 hours to compare their mechanical properties with those of clays prepared with CSP. After sintering at 1100 °C, the highest compressive strength was obtained with Cl, which also had the highest density (2.27 g/cm^3) and the lowest porosity (~11%). Illite with comparable density (2.21 g/cm^3) and porosity (~14 %) achieved a twice lower compressive strength (161 MPa), while kaolinite showed significantly lower compressive strengths with values from 6 to 36 MPa. The lower values for the compressive strength of kaolinite can be attributed to the fact that the optimum sintering temperature was not reached at this temperature. After sintering at 1300 °C, the low-defect kaolinite achieved the highest compressive strength (341 MPa) with low porosity (4.6 %) and high density (2.58 g/cm^3). In a preliminary analysis, we have also shown the promising results of CSP.

Acknowledgments

The authors thank Dr. Lea Žibret for the particle size distribution measurements, Dušica Tauzes for the XRF measurements and Dr. Lidija Korat and Roman Maček for microXCT images and 3D reconstructions (all from the Laboratory for Cements, Mortars and Ceramics, ZAG). This work was supported by the Slovenian Research Agency through the project No. J1-3026 »Applicability of the cold sintering process to clay minerals«.

References

Balan, E., Calas, G., Bish, D.L. (2014). Kaolin-Group Minerals: From Hydrogen-Bonded Layers to Environmental Recorders, Elements, 10(3), 183–188. doi: 10.2113/gselements.10.3.183

Galotta, A., Sglavo, V.M. (2021). The cold sintering process: A review on processing features, densification mechanisms and perspectives, Journal of the European Ceramic Society, 41(16), 1-17. doi: 10.1016/j.jeurceramsoc.2021.09.024.

Gianni, E., Avgoustakis, K., Papoulis, D. (2020). Kaolinite group minerals: Applications in cancer diagnosis and treatment, European Journal of Pharmaceutics and Biopharmaceutics,154, 359-376. doi: 10.1016/j.ejpb.2020.07.030.

Grasso, S., Biesuz, M., Zoli, L., Taveri, G., Duff, A.I., Ke, D., Jiang, A., Reece, M.J. (2020). A review of cold sintering processes, Advances in Applied Ceramics, 119(3), 115-143. doi: 10.1080/17436753.2019.1706825.

Guo, H., Baker, A., Guo, J., Randal, C.A. (2016). Cold Sintering Process: A Novel Technique for Low-Temperature Ceramic Processing of Ferroelectrics, Journal of the American Ceramic Society, 99(11), 3489-3507. doi: 10.1111/jace.14554.

Maria, J.P, Kang, X., Floyd, R.D., Dickley, E.C., Guo, H., Guo, J., Baker, A., Funihashi, S., Randall C.A. (2017). Cold sintering: Current status and prospects, Journal of Materials Research, 32(17), 3205–3218. doi:10.1557/jmr.2017.262.

Michot, A., Smith, D.S., Degot, S., Gault, C. (2008). Thermal conductivity and specific heat of kaolinite: Evolution with thermal treatment, Journal of the European Ceramic Society, 28(14), 2639-2644. doi: 10.1016/j.jeurceramsoc.2008.04.007.

Zhang, S., Sutejo, I.A., Kim, J., Choi, Y.-J., Park, H., Yun, H.-S. (2022). Three-dimensional complex construct fabrication of illite by digital light processing-based additive manufacturing technology, Journal of the American Ceramic Society, 105(6), 3827–3837. doi: 10.1111/jace.18369.